^{18}F-FDG metabolism in a rat model of chronic infarction

A 17-sector semiquantitative analysis

I. Peñuelas[1,2], G. Abizanda[3,4], M. J. García-Velloso[1], J. J. Gavira[5], J. M. Martí-Climent[1], M. Ecay[2], M. Collantes[2], J. A. García de Jalón[6], A. García-Rodríguez[6], M. Mazo[3,4], J. Barba[5], J. A. Richter[1], F. Prósper[3,4]

Department of [1]Nuclear Medicine, [3]Hematology and Cell Therapy Service, [5]Cardiology and Cardiovascular Surgery, Clínica Universitaria, [4]Foundation for Applied Medical Research, University of Navarra, [2]MicroPET Research Unit CIMA-CUN, Pamplona, Spain,
[6]Department of Animal Pathology, Veterinary Faculty, University of Zaragoza, Spain

^{18}F-FDG-Metabolismus im Rattenmodell für chronischen Infarkt: Eine semiquantitative Analyse mit 17 Sektoren

Keywords
Myocardial infarction, ^{18}F-FDG-microPET, parametric polar map

Summary
Strategies to establish the functional benefit of cell therapy in cardiac regeneration and the potential mechanism are needed. **Aims:** Development of a semi-quantitative method for non invasive assessment of cardiac viability and function in a rat model of myocardial infarction (MI) based on the use of microPET. **Animals, methods:** Ten rats were subjected to myocardial imaging 2, 7, 14, 30, 60 and 90 days after left coronary artery ligation. Intravenous ^{18}F-fluoro-2-deoxy-2-D-glucose (^{18}F-FDG) was administered and regional ^{18}F activity concentrations per unit area were measured in 17 regions of interest (ROIs) drawn on cardiac polar maps. By comparing the differences in ^{18}F uptake between baseline and each of the follow up time points, parametric polar maps of statistical significance (PPMSS) were calculated. Left ventricular ejection fraction (LVEF) was blindly assessed echocardiographically. All animals were sacrificed for histopathological analysis after 90 days. **Results:** The diagnostic quality of ^{18}F-FDG microPET images was excellent. PPMSS demonstrated a statistically significant decrease in ^{18}F concentrations as early as 48 hours after MI in 4 of the 17 ROIs (segments 7, 13, 16 and 17; $p < 0.05$) that persisted throughout the study. Semiquantitative analysis of ^{18}F-FDG uptake correlated with echocardiographic decrease in LVEF ($p < 0.001$). **Conclusion:** The use of PPMSS based on ^{18}F-FDG-microPET provides valuable semi-quantitative information of heart glucose metabolism allowing for non-invasive follow up thus representing a useful strategy for assessment of novel therapies in cardiac regeneration.

Nuklearmedizin 2007; 46: 149–154
doi: 10.1160/nukmed-0065

Schlüsselwörter
Myokardinfarkt, ^{18}F-FDG-Kleintier-PET, parametrische Polar-Map

Zusammenfassung
Strategien zur Ermittlung des funktionellen Nutzens einer Zelltherapie zur kardialen Regeneration und der potenziellen Mechanismen werden benötigt. **Ziele:** Entwicklung eines semiquantitativen Verfahrens zur nicht invasiven Bestimmung der kardialen Vitalität und Funktion in einem Rattenmodell für Myokardinfarkt (MI) basierend auf der Untersuchung mittels microPET. **Tiere, Methodik:** Bei zehn Ratten erfolgte 2, 7, 14, 30, 60 und 90 Tage nach einer Ligatur der Arteria coronaria sinistra eine myokardiale Bildgebung. ^{18}F-Fluor-2-deoxy-2-D-glukose (^{18}F-FDG) wurde intravenös verabreicht und die regionalen ^{18}F-Aktivitätskonzentrationen pro Gebiet in 17 ROIs (regions of interest), die auf Polar-Maps definiert wurden, gemessen. Mittels eines Vergleichs der Differenzen der Aufnahme von ^{18}F zwischen dem Ausgangswert und jedem der Zeitpunkte der Nachbeobachtung wurden parametrische Polar-Maps der statistischen Signifikanz (parametric polar maps of statistical significance, PPMSS) berechnet. Die linksventrikuläre Ejektionsfraktion (LVEF) wurde geblindet echokardiographisch untersucht. Alle Tiere wurden nach 90 Tagen zur histopathologischen Analyse getötet. **Ergebnisse:** Die diagnostische Qualität der ^{18}F-FDG-microPET-Bilder war ausgezeichnet. In den PPMSS zeigte sich bereits 48 Stunden nach dem MI eine statistisch signifikante Verringerung der ^{18}F-Konzentrationen in vier der 17 ROIs (Segmente 7, 13, 16 und 17; $p < 0{,}05$), die während der gesamten Studie persistierte. Die semiquantitative Analyse der ^{18}F-FDG-Aufnahme korrelierte mit der echokardiographischen Verringerung der LVEF ($p < 0{,}001$). **Schlussfolgerung:** Die Verwendung von PPMSS auf Basis der ^{18}F-FDG-microPET ergibt wertvolle semiquantitative Informationen des kardialen Glukosemetabolismus und ermöglicht die nicht invasive Nachbeobachtung. Sie ist nützlich zur Beurteilung der Wirksamkeit neuer Therapien zur kardialen Regeneration.

Myocardial infarction (MI) and its consequence heart failure is the leading cause of death in the developed countries. Translational cardiovascular research increasingly relies on the use of small animals like rats and mice (4, 13). However, examination of rodent heart function in vivo remains challenging because of its small size. The availability of properly validated techniques that might permit repeated non-invasive measurement of heart function in detail would be of enormous value in cardiovascular research for the evaluation of novel pharmaceutical, cellular and gene therapy based therapies. The development of high-resolution small animal-dedicated PET scanners has opened new perspectives on the use of PET imaging of myocardial function in rodents. In the study of rat heart, these so-called microPET devices are most recently being used for cardiac transgene expression studies (2, 6) although there is also great interest in the detailed analysis of rat myocardial innervation and metabolism with microPET (3, 8).

This study was designed to non-invasively assess, in a chronic rat model of MI whether there was spontaneous recovery of myocardial glucose metabolism during long-term (up to three months) follow up using ^{18}F-FDG-microPET for assessment of cardiac function. We carried out detailed 17-sector semi-quantitative analysis of myocardial ^{18}F-FDG uptake and analyzed the evolution of the infarction by means of PPMSS. We demonstrate that the use of ^{18}F-FDG-microPET provides valuable semi-quantitative information and allow non-invasive follow up

Received: November 3, 2006; accepted in revised form: March 7, 2007

of heart glucose metabolism, representing a useful strategy for assessment of novel therapies in cardiac regeneration.

Animals, material, methods

Model for myocardial infarction

Sprague-Dawley rats (Harlan Interfauna IBERICA S.L) weighing 200 to 250 g were used in this study. Chronic myocardial infarction was induced by ligation of the left anterior descending coronary artery as previously described (1). All animal procedures were approved by the University of Navarra Institutional Committee on Care and Use of Laboratory Animals.

PET imaging, image reconstruction, and semiquantitative evaluation

Animals had water and food ad libitum until the begin of the PET study, as we have previously found that such conditions along with a long uptake time (120 min) of the radiopharmaceutical yield the best microPET images of ^{18}F-FDG heart uptake. Rats were momentarily anaesthetized with 2% isoflurane in 100% O_2 gas for ^{18}F-FDG injection (75 MBq in 100–200 µl) in a tail vein. Two hours after tracer injection, animals were anesthetized with isoflurane, placed prone on the PET scanner cradle and kept during the overall study under continuous influx of the anesthetic.

A static 60-minute sinogram was acquired in a Mosaic (Philips) small animal dedicated imaging tomograph as we have previously described (10). No transmission scan was performed. Ten animals were repeatedly imaged using similar conditions at different time points: before the MI, and 2, 7, 14, 30, 60 and up to 90 days later.

Sinograms were reconstructed using the 3D-Ramla algorithm – a true 3D-reconstruction – with two iterations and a relaxation parameter of 0.024, into a 128×128 matrix with a 1 mm voxel size (12). Scanner efficiency normalization, dead time and decay corrections were applied during reconstruction. Images were reoriented for further processing and polar maps obtained using the specific cardiac imaging software package of the PET scanner. The area of each of the sectors does not correspond to any anatomical area, but it can be seen as a simplified representation of volumes of tissue located in different planes along the heart axis. The bigger the volume considered the bigger the area of the sector. Furthermore, the areas are defined following the same areas that are used to calculate the wall motion score index regional contractility using echocardiography analysis. The standard and 17-segment cardiac grid widely used in cardiology assessment (Fig. 1) was superimposed on each of the polar maps displays and 17 regions of interest (ROIs) drawn accordingly (10). So in that sense the division in 17 segments is validated by their wide use in cardiology assessment.

Individual quantification of the ^{18}F-FDG uptake in each of them was calculated. The total number of counts obtained for each of the ROIs was divided by its corresponding area to obtain counts per area unit. For each PET study, the maximal value of the 17 ROIs was considered as 100% and the remaining data so transformed into percentage values. All further calculations and statistical analysis were performed on these sets of re-scaled numerical data.

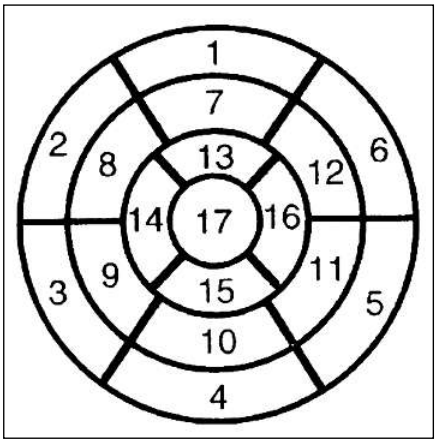

Fig. 1 Polar map with 17 regions of interest for measuring regional myocardial ^{18}F activity concentrations:
segments 1, 7, 13: basal (1), mid (7), and apical (13) anterior segments, the
segments 4, 10, 15: basal (4), mid (10), and apical (15) inferior segments,
septum (5 segments): basal anteroseptal (2), basal inferoseptal (3), mid anteroseptal (8), mid inferoseptal (9), and apical septal (14).
The lateral wall is divided into the basal anterolateral (6), basal inferolateral (5), mid anterolateral (12), mid inferolateral (11), and apical lateral (16). The long-axis segment is called apex (17).

Relative values were used trying to make the quantification procedure simpler, as they are the same if derived from raw data (without taking into account the calibration tables of the PET scanner), from radioactivity concentration or from SUV values. For the two latter cases, a calibration of the PET scanner is mandatory to convert raw data into Bq/cc.

By using ratios, results are not dependant on the calibration factor of the equipment that as it is well established are very different depending on the size (diameter) of the phantom used for such calibration. Hence, differences in the size of the animals used (that could of course occur as the study lasted for three months) would not affect the results.

Echocardiography, histopathology

Two-dimensional echocardiography, M-mode recordings, and Doppler ultrasound measurements were performed using a Sonos 4500 ultrasound system (Philips) with a 12 MHz linear array transducer as described (1). Echocardiographic studies were performed at baseline (before infarct), and 14, 30, 60 and up to 90 days later. All the studies were done by the same investigator. Measurements were done in three cycles and the mean value was obtained. The coefficient of variation (CV) was 4.5% for LV end-diastolic volume and CV 7.6% for LVEF.

Animals were sacrificed for histopathological studies 90 days after infarction in a CO2 chamber. Hearts were explanted and fixed in 10% formaldehyde solution. Six 2 mm thick transversal sections were obtained and were routinely processed and embedded in paraffin. Paraffin-embedded blocks were cut into 4 µm sections and stained with haematoxilin and eosin, Gallego's trichrome method and Sirius red staining (7).

Statistics

Statistical analysis was performed with the SPSS 13.0 for windows software package. Comparisons were performed using the paired and unpaired t test when appropriate, once normality was demonstrated with the Shapiro-Wilk and Kolmogorov-Smirnov normality test. In case of non-normal dis-

tribution, Wilcoxon test was used. Comparisons for repeated measurements were performed with ANOVA or Friedman test. Lineal regression analysis was performed using Pearson correlation coefficients. Descriptive analysis is presented as mean (SEM) for quantitative variables or median (IQR) for categorical variables. Differences were considered statistically significant when $p < 0.05$.

Results

Image quality and semiquantitative values

The two hour ^{18}F-FDG uptake protocol rendered images of excellent diagnostic quality, with a high myocardial uptake of the tracer and a very low background (Fig. 2). Such good quality images were obtained in all the studies, and no image was deemed as non-evaluable. Furthermore, the liver uptake was very low, thus avoiding possible problems of artificially increasing the ^{18}F activity on the inferior wall of the heart.

The ^{18}F-FDG uptake in the baseline state of the different segments was not uniform with slightly higher uptake observed in the basal and mid anterior segments, basal anteroseptal, mid anteroseptal, mid inferoseptal and apical septal segments. However, a similar uptake pattern was obtained for a specific ROI in all animals studied, with very small variability between animals (Tab. 1,Fig. 3).

^{18}F-FDG uptake after infarction

A significant decrease in ^{18}F-FDG uptake in certain segments was patent in the micro-PET-^{18}F-FDG images as soon as 48 h after the infarction, and persisted during the three months of follow up (Fig. 3).

To determine whether any single segment showed either a decreased or increased ^{18}F-FDG uptake after the MI, we performed segment by segment individual comparisons at each time point with baseline ^{18}F-FDG uptake (Fig. 4). Moderate to severe decrease in myocardial metabolism was observed in the apex, apical anterior and apical lateral segments. Such decreases initiated very early after MI. Myocardial metabolism in apical inferior and apical septal segments was also decreased but to a lesser extent. Interestingly, the mid anterolateral segment initially shows a pronounced reduction in ^{18}F-FDG uptake that was reversed two weeks after MI and remained stable throughout the rest of the study.

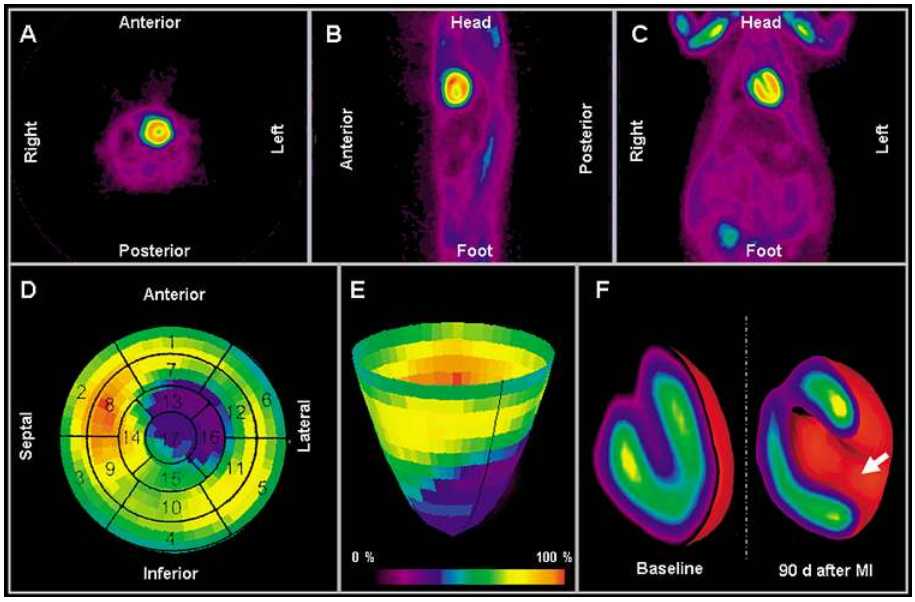

Fig. 2 MicroPET imaging of ^{18}F-FDG heart uptake: Transverse (A), sagittal (B) and coronal (C) 2 mm-thick images obtained in an animal at baseline before the MI. A very low background and an intense heart uptake permit a good delineation of the organ. (D) Polar map of the myocardial ^{18}F-FDG uptake obtained from a representative animal 2 days after the MI. The 17-segment grid has been superimposed to define the ROIs used for the analysis. (E) Cone-revolution 3D representation of the polar map. (F) Three dimensional rendering of the left ventricle derived from the polar coronal images of the heart. Lack of ^{18}F-FDG uptake in the sectors affected by the infarct produces a hole-like image in the corresponding region (arrow) as compared with the non-infarct heart.

Statistical significance

For proper statistical assessment of differences between segments along the study, non-parametric Wilcoxon tests for paired samples were performed to compare each of the segments with the baseline state and to facilitate the interpretation of the statistical calculations, we generated PPMSS (Fig. 3). Such parametric maps were made by coloring on the 17-sector grid those sectors in which statistically significant differences between the basal state and the corresponding time were found. In Figure 3, we can see the comparison of each of the segments in the different PET studies along time with the myocardial ^{18}F-FDG uptake in each seg-

Tab. 1 Myocardial ^{18}F-FDG uptake for each ROI (sector). Uptake is homogeneous in all the sectors before the infarction. Mean (%) and variation coefficients (VC) of ^{18}F-FDG uptake at baseline is shown for each of the seventeen sectors.

sector #	mean (%)	VC (%)
1	92.5	5.2
2	93.9	6.0
3	85.8	6.8
4	76.7	6.5
5	81.4	7.1
6	83.0	4.9
7	95.9	4.8
8	98.8	2.0
9	92.3	3.6
10	84.4	6.0
11	85.8	1. 0
12	87.2	6.2
13	88.5	5.3
14	91.5	5.5
15	80.4	8.5
16	79.7	8.4
17	82.4	7.7

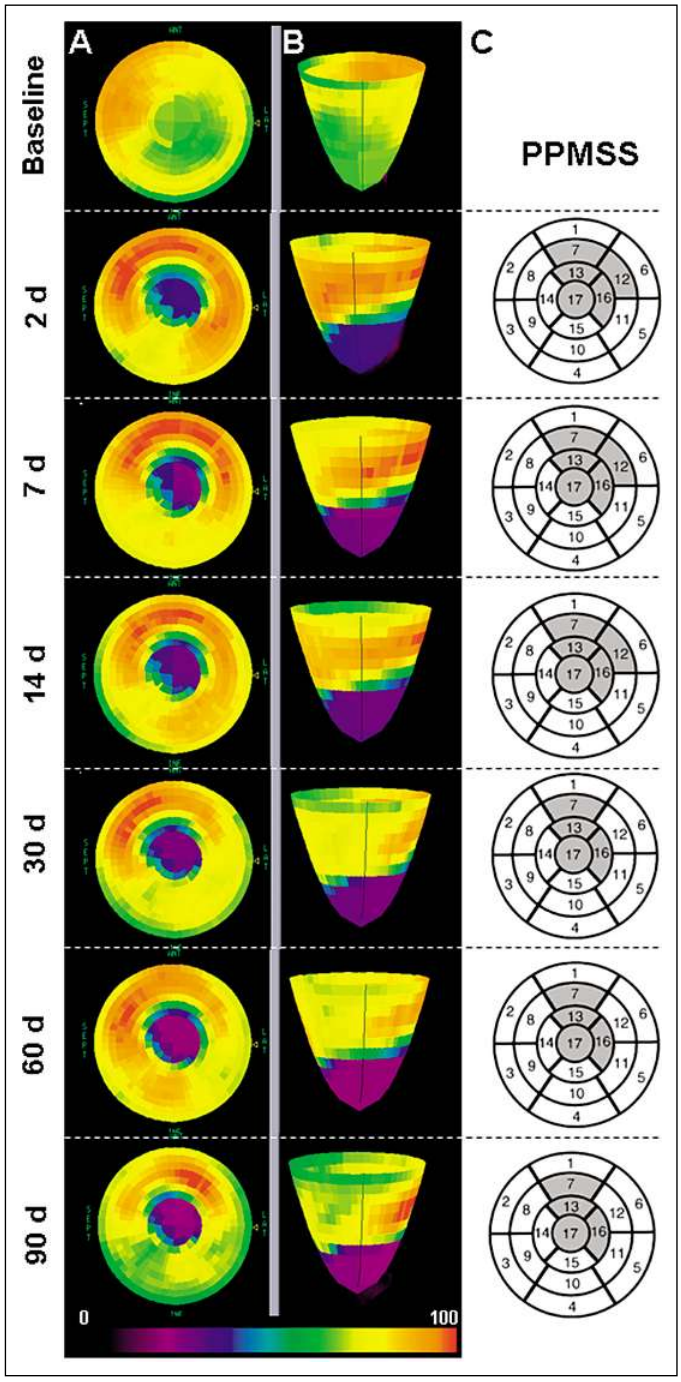

Fig. 3 Evolution of the MI shown by ^{18}F-FDG myocardial uptake
(A, B) Polar maps and three dimensional cone-revolution reconstructions of the microPET scans made before the infarction and 2, 7, 14, 30, 60 and 90 days after it. All images correspond to studies performed to the same animal. Color bar represents percentage uptake.
(C) Corresponding PPMSS (parametric polar maps of statistical Significance): Shadowed sectors represent those in which statistical significant differences were found between the corresponding time point and the baseline (see text).

ment before the MI. These PPMSS provide a topographical image of differences between segments that can help understand the progression of the infarct and to determine whether there is spontaneous recovery of ^{18}F-FDG myocardial uptake after MI. According to the PPMSS, a statistically significant ($p < 0.05$) decrease in the apex, apical anterior, apical lateral and mid anterior segments (17, 13, 16 and 7, respectively) was observed. Such diminution was already observed two days after MI and increased progressively during the three months follow up. The mid anterolateral segment (number 12) initially showed a statistically significant ($p<0.05$) decrease at days 2 and 7 but then recovered by day 14 (Fig. 4, Fig. 5).

Echocardiography, histopathology

The effect of MI in the left ventricular function was analyzed by echocardiography. As expected, there was a marked reduction in LVEF from baseline (68.5 ± 1.1) to 14 days post infarct (38.3 ± 4.1) with a further decrease at 30, 60 and 90 days (36.9 ± 3.0; 33.8 ± 2.5; 32.1 ± 2.93 respectively) ($p < 0.05$) (Tab. 2). The effect on cardiac remodeling after MI was also quantified by assessment of ventricular volumes and diameters, demonstrating a statistically significant increase in LV end-systolic and diastolic volumes and diameters ($p < 0.05$) (Tab. 2). A correlation between LVEF and the decrease in ^{18}F-FDG ($r = 0.85$; $p < 0.001$, $r = 0.95$; $p < 0.01$ for 17 and 4 segments respectively) was observed (Fig. 5).

Finally, to determine the association between histological and ^{18}F-FDG uptake findings analyzed by microPET we visually compared the size and location of the MI area in the postmortem tissue and the corresponding polar map region (Fig. 6). The infarct area was clearly identified macroscopically showing a progressive slimming of the left ventricle wall in the medial and apical regions, corresponding to the functional ^{18}F-FDG uptake defect affecting the apex, apical anterior, apical lateral and mid anterior segments (17, 13, 16 and 7, respectively).

Discussion

Doppler measurement of rat heart function is relatively easy, but does not allow for a detailed sector by sector analysis as the one we have carried out using microPET and dividing the polar map into 17 sectors. Although the possibility to non-invasively analyze in detail the radioactivity accumulation in the rat heart at high resolution by microPET imaging has been previously validated (8), in this study we develop a semiquantitative analysis that allows the evaluation of cardiac metabolism and the assessment and quantization of cardiac defects associated with myocardial infarction. This model based on the analysis of 17-segments or ROIs facilitates the time dependent follow up of cardiac function as well as the evaluation of the effect of novel therapies. As it is not foreseeable to have large increases in myocardial metabolic activity after such treatments, a gross visual scale (5) would be of little value,

so to have the chance to correctly evaluate a possible response, detailed quantitative or semiquantitative analysis as the one described should be necessary.

The reason not to use attenuation correction of the microPET image in our study is two fold: from a practical point of view, transmission scans with the available sources for microPET imaging devices imply a substantial increase of the overall microPET protocol duration, as they require a prolonged period of time. In addition, Kudo et al. (8) have demonstrated that correction for photon attenuation has no systematic effect on activity concentrations in any myocardial regions in the study of ^{18}F activity in rat heart. These authors have shown that activity concentrations derived from corrected and uncorrected images correlate linearly with the true activity concentrations. Furthermore, the use of uncorrected images did not affect the coefficients of variation of ^{18}FDG activity concentration in the myocardium (8).

Tracer kinetic modeling used in conjunction with PET can ideally be used for non-invasive quantization of physiological, biological and molecular processes and their alterations due to disease. However, techniques that have been established and validated to serially measure blood activity concentrations in humans need to be carefully revised for animal experiments, especially for small animals such as rats. In rodents the vascular access is quite problematic, the heart rate very high and the blood volume usually a limiting factor (9). Consequently, the possibility to perform absolute quantization of ^{18}FDG myocardial uptake in small laboratory animals, although feasible is complex. Taking into account the long protocol we have used (120 min uptake and 60 min imaging), for proper absolute quantization of FDG myocardial uptake, a 3 h period of anaesthesia would have been required. In addition, an absolute quantitative model using blood sampling is very invasive for rodents and might probably not even be feasible when a single animal has to undergo many PET studies in a short time interval, as is our case. Furthermore, repeatedly withdrawing a certain volume of blood for radioactivity analysis in severely infarct animals might probably alter the natural evolution of the lesion and somehow mask the results.

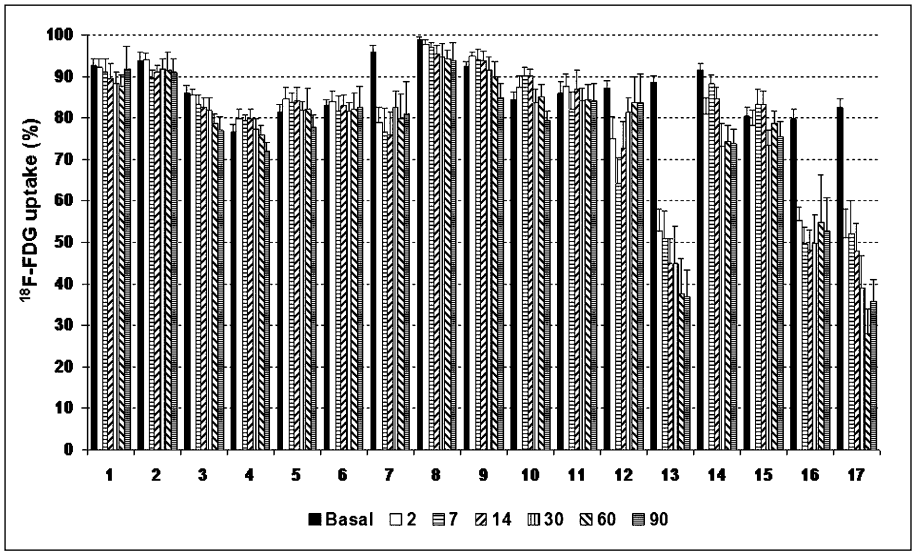

Fig. 4 Semiquantitative values of radioactivity accumulation: ^{18}F-FDG normalized uptake calculated at baseline and 2, 7, 14, 30, 60 and 90 days after MI for each of the 17 segments. Each bar represents the mean ± SEM of ^{18}F-FDG uptake of all animals.

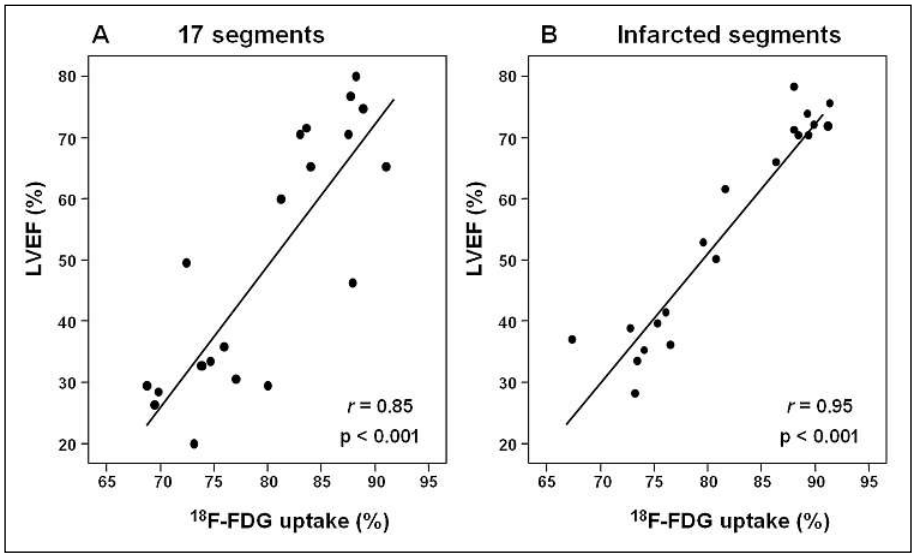

Fig. 5 Correlation between LVEF and ^{18}F-FDG uptake: Semiquantitative values of radioactivity accumulation calculated as the mean value of the FDG uptake of the 17 sectors together (A) ($r = 0.85$; $p < 0.001$) or the median uptake of the infarcted segments (B) at baseline and premortem ($r = 0.95$; $p < 0.01$) were statistically correlated with LVEF.

Tab. 2 Echocardiographic parameters (mean ± SEM; *$p < 0.05$ versus baseline)
LVEF: left ventricular ejection fraction; LVEDV: left ventricular end-diastolic volume; LVESV: left ventricular end-systolic volume; LVEDD: left ventricular end-diastolic diameter; LVESD: left ventricular end-systolic diameter

	LVEF (%)	LVEDV (ml)	LVESV (ml)	LVEDD (mm)	LVESD (mm)
baseline	68.5 ± 1.1	0.47 ± 0.038	0.152 ± 0.015	0.576 ± 0.017	0.381 ± 0.015
15 days	38.3 ± 4.1*	0.778 ± 0.122	0.493 ± 0.095*	0.674 ± 0.046	0.563 ± 0.044*
30 days	36.9 ± 3*	1.043 ± 0.127*	0.695 ± 0.103*	0.755 ± 0.022*	0.646 ± 0.036*
60 days	33.8 ± 2.5*	0.999 ± 0.077*	0.681 ± 0.070*	0.758 ± 0.022*	0.651 ± 0.028*
90 days	32.1 ± 2.9*	1.151 ± 0.081*	0.814 ± 0.075*	0.797 ± 0.023*	0.691 ± 0.027*

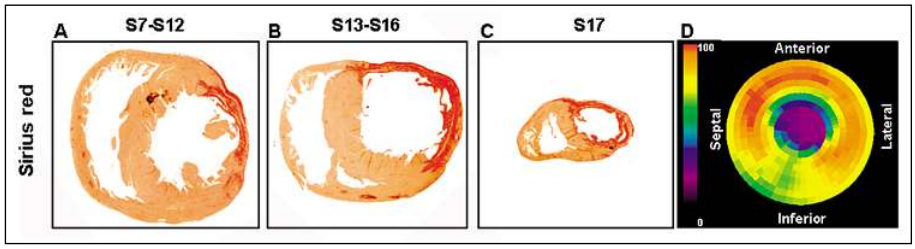

Fig. 6 Postmorten histopathological correlation with in vivo PPMSS: Representative picrosirius red–stained sections of postmortem myocardial slices of infarct area from a rat sacrificed 90 days after MI corresponding to segments 7–12 (A), 13–16 (B), and 17 (C) from the polar map and the corresponding polar map showing decreased ^{18}F-FDG uptake in apex, apical anterior, apical lateral and mid anterior segments (17, 13, 16 and 7) (D). Collagen stains red in the area corresponding to segment 7 and 12 (A), 13 and 16 (B) and 17 (C) while normal cardiac muscle stains yellow.

As expected for a model of MI, myocardial ^{18}F-FDG uptake was significantly reduced in the affected segments very early. As soon as 48 hours after the infarction the activity in segments 13, 16, 17 and 7 (apical anterior, apical lateral, apex and mid anterior) was reduced down to values around 50%. On the other hand, the ^{18}F-FDG uptake in segment 12 (mid anterolateral) showed a statistical significant reduction in the PET images obtained at day 2 and at day 14 post-infarction, but the myocardial ^{18}F-FDG metabolism was recovered by day 30 as compared to the basal state. We cannot consider this phenomenon the result of a spontaneous recovery after reperfusion of an infarct area but probably related to myocardial stunning. Decreased ^{18}F-FDG uptake maybe observed after myocardium stunning and may increase once myocardial function has been recovered. This may be the case for the observed recovery of ^{18}FDG uptake in segment 12. Due to the impossibility of measuring regional contractility by echocardiography for each segment, we cannot establish whether segment 12 recovered normal function, and hence it might have been classified as a „stunning" sector.

Importantly, the semiquantitative analysis of ^{18}F-FDG uptake showed a strong correlation with LVEF measured by echocardiography both when only those segments with decreased viability were analyzed but also when the decrease in uptake was diluted by analyzing all 17-segments. Although LVEF is a measure of global heart function the amount of non-viable tissue correlates with the functional capacity of the heart and validates our approach as a measurement of cardiac function.

Making a 17-sector analysis might seem too coarse, but once the methodology has been established, making either a 5, 11 or 17-sector analysis does not make a significant difference. On the other hand, if the experimental therapeutic intervention used for (partial) recovery of infarction gives a small response, a 17-sector analysis might permit seeing the result, while a less detailed analysis may neglect finding small but significant differences due to an averaged value from affected and non-affected sectors.

It is important to point out that the correlation between the infarct area determined histopathologically and the segments with decreased ^{18}F-FDG uptake was performed visually and do not represent a formal statistical correlation between infarct size and ^{18}F-FDG uptake.

Conclusion

We have demonstrated the possibility to analyze and quantify in detail the radioactivity accumulation and glucose metabolism in the rat heart by microPET imaging and used this technique in a small animal model of MI. This technique offers the possibility of not invasively follow up of heart glucose metabolism thus representing a useful strategy for assessment of different therapies (i. e. gene therapy, stem cell based approaches) in cardiac regeneration and screening for novel drugs designed to reduce acute damaged to the myocardium after ischaemia.

Acknowledgement

Supported in part by grants from Fondo de Investigaciones Sanitarias PI042125, Ministerio de Ciencia y Tecnologia SAF2002–04575-C02–02, FEDER (INTERREG IIIA) and RTICCC C03/10. This project was funded in part through the „UTE project CIMA". We appreciate the technical assistance of Javier Guillén, Beatriz Pelacho, the cyclotron and radiopharmaceutical synthesis team.

References

1. Agbulut O, Mazo M, Bressolle C et al. Can bone marrow-derived multipotent adult progenitor cells regenerate infarcted myocardium? Cardiovasc Res 2006; 72: 175–183.
2. Chen IY, Wu JC, Min JJ et al. Micro-positron emission tomography imaging of cardiac gene expression in rats using bicistronic adenoviral vector-mediated gene delivery. Circulation 2004; 109: 1415–1420.
3. Croteau E, Benard F, Cadorette J et al. Quantitative gated PET for the assessment of left ventricular function in small animals. J Nucl Med 2003; 44: 1655–1661.
4. Hasenfuss G. Animal models of human cardiovascular disease, heart failure and hypertrophy. Cardiovasc Res 1998; 39: 60–76.
5. Hernandez-Pampaloni M, Allada V, Fishbein MC et al. Myocardial perfusion and viability by positron emission tomography in infants and children with coronary abnormalities: correlation with echocardiography, coronary angiography, and histopathology. J Am Coll Cardiol 2003; 41: 618–626.
6. Inubushi M, Wu JC, Gambhir SS et al. Positron-emission tomography reporter gene expression imaging in rat myocardium. Circulation 2003; 107: 326–332.
7. Junqueira LC, Bignolas G, Brentani RR. Picrosirius staining plus polarization microscopy, a specific method for collagen detection in tissue sections. Histochem J 1979; 11: 447–455.
8. Kudo T, Fukuchi K, Annala AJ et al. Noninvasive measurement of myocardial activity concentrations and perfusion defect sizes in rats with a new small-animal positron emission tomograph. Circulation 2002; 106: 118–123.
9. Laforest R, Sharp TL, Engelbach JA et al. Measurement of input functions in rodents: challenges and solutions. Nucl Med Biol 2005; 32: 679–685.
10. Marti-Climent JM, Garcia Velloso MJ, Serra P et al. Positron emission tomography with PET/CT. Rev Esp Med Nucl 2005; 24: 60–76.
11. Schelbert HR, Beanlands R, Bengel F et al. PET myocardial perfusion and glucose metabolism imaging: Part 2: Guidelines for interpretation and reporting. J Nucl Cardiol 2003; 10: 557–571.
12. Surti S, Karp JS, Perkins AE et al. Imaging performance of A-PET: a small animal PET camera. IEEE Trans Med Imaging 2005; 24: 844–852.
13. Verdouw PD, van den Doel MA, de Zeeuw S et al. Animal models in the study of myocardial ischaemia and ischaemic syndromes. Cardiovasc Res 1998; 39: 121–135.

Correspondence to:
Iván Peñuelas, PhD
Department of Nuclear Medicine
Clínica Universitaria de Navarra, Av Pio XII 36
31008 Pamplona, Spain
Tel. +34/9 48/25 54 00
Fax +34/9 48/29 65 00
E-mail: ipenuelas@unav.es